J. Mol. Biol. (1981) **145**, 735–756

DNA Sequence Changes of Mutations Altering Attenuation Control of the Histidine Operon of *Salmonella typhimurium*

H. MARK JOHNSTON†

AND

JOHN R. ROTH

Department of Biology
University of Utah
Salt Lake City, Utah 84112, U.S.A.

(Received 10 July 1980)

The DNA sequence changes of 31 mutations altering the attenuation control mechanism of the histidine operon are presented. These mutations are discussed in terms of a model for operon regulation that involves a *his* leader peptide gene whose translation regulates formation of alternative stem-loop structures in the *his* leader messenger RNA. Three suppressible mutations generate nonsense codons (ochre and UGA) in the *his* leader peptide gene, demonstrating that translation of this gene is essential for operon expression. Eight mutations presumably reduce the efficiency of translation initiation of the *his* leader peptide gene, causing reduced levels of operon expression. Five of these mutations directly alter the leader peptide gene initiator codon (AUG). Three mutations alter sequences just in front of the initiator codon and presumably alter the ribosome recognition site. Fourteen mutations reduce the stability of the *his* leader mRNA stem-loop structures that are alternatives to the attenuator stem. The properties of these mutations provide support for the role of these stem-loop structures in preventing formation of the attenuator stem. Finally, we show that mutations that alter the attenuator stem suppress *hisO* mutations. This lends support to the proposal that these *hisO* mutations cause reduced levels of operon expression due to excessive attenuator stem formation. The properties of these 31 mutations provide substantial support for the model of *his* operon regulation described in this paper.

1. Introduction

Gene expression in prokaryotes seems to be regulated in most cases at the level of transcription. One major regulatory mechanism, for which the *lac* operon is the prototype, involves the regulation of the frequency of transcription initiation by repressor or activity proteins (see Miller & Reznikoff, 1978 for reviews). A fundamentally different regulatory mechanism, involving the regulation of transcription terminations, has recently been revealed (Kasai, 1974; Bertrand

† Present address: Department of Biochemistry, Stanford University Medical School, Palo Alto, Calif. 94305, U.S.A.

0022-2836/81/040735-22 $02.00/0

et al., 1975; see Adhya & Gottesman, 1978 for review). This type of mechanism is responsible for the regulation of expression of several bacterial operons encoding amino acid biosynthetic enzymes (Bertrand *et al.*, 1975; Zurawski *et al.*, 1978*a*; Oxender *et al.*, 1979; Keller & Calvo, 1979; Gardiner, 1979; Gemmill *et al.*, 1979; Lawther & Hatfield, 1980) including the histidine operon of *Salmonella typhimurium* (Kasai, 1974; Barnes, 1978*b*).

Under conditions of excess histidine availability, *his* operon transcription terminates at a site in the *his* control region called the attenuator. When cells are starved for histidine, transcription proceeds through this attenuator site and into the *his* structural genes (Kasai, 1974). This event is due to low intracellular levels of histidyl-tRNA (Lewis & Ames, 1972), and requires translation of the *his* control region (Artz & Broach, 1975). The DNA sequence of the *his* operon control region reveals two major features important to this regulatory mechanism: (1) a G+C-rich region of dyad symmetry followed by an A+T-rich region that is thought to be the attenuator site where *his* transcription normally terminates, and (2) proximal to the attenuator site, a small gene 51 bases in length containing seven histidine codons in tandem (Barnes, 1978*b*; DiNocera *et al.*, 1978). The rate of translation of this small gene is sensitive to histidyl-tRNA levels in the cell, and is thought to regulate termination of transcription at the attenuator site (Barnes, 1978*b*; DiNocera *et al.*, 1978).

We have proposed a detailed model for the mechanism of *his* operon regulation (Johnston *et al.*, 1980). Supporting evidence for this model comes primarily from the characterization of a large number of mutations in the *his* control region (*hisO*) causing reduced operon expression (Johnston & Roth, 1980). To identify the region in the DNA sequence affected by these mutations, and to understand the basis of the effects of these mutations on *his* operon regulation, we determined the DNA sequence changes in many of these *hisO* mutants. In this paper the DNA sequence changes of these mutations are presented and their implications for the mechanism of *his* operon regulation are discussed in detail.

2. Material and Methods

(a) *Genetic techniques using the M13*-hisOGD *hybrid phage*

The M13-*hisOGD* hybrid phage constructed by Barnes (1979; referred to as M13Hol76), was the source of *hisO* DNA for sequencing. This phage carries a 3300 base-pair insert in the M13 intergenic region and contains the *hisO*, *hisG* and *hisD* genes (Barnes, 1979). This phage is able to infect F′-containing strains of *S. typhimurium*, and can confer on them the ability to grow on histidinol (*hisD*$^+$). To introduce *hisO* mutations onto the phage for sequencing, we developed the following *in vivo* technique to detect M13 phage that have undergone recombination with the chromosome (Bossi & Johnston, unpublished results). M13Hol76 carrying a *hisD*$^-$ mutation (Bossi & Roth, 1980), was used to infect a *hisO* mutant strain carrying an F′. Infected cells carrying the M13Hol76 (replicative form) are His$^+$, presumably due to complementation. Many His$^+$ colonies were picked, pooled, and the M13Hol76 phage they released collected by centrifugation of the bacterial suspension, followed by heating the supernatant to 70°C for 20 minutes to kill any remaining bacteria (M13 is relatively stable to this treatment). These phage were used to infect a *his* deletion mutant lacking the *hisD* gene, selecting growth on histidinol (*hisD*$^+$). Since the input phage are *hisD*$^-$, only recombinant or revertant (*hisD*$^+$) phage should transduce this recipient to

Hol$^+$. Among the Hol$^+$ transductants, those that carry an M13Hol76 containing the linked *hisO* mutation can be identified. In most cases, 50 to 100% of the *hisD*$^+$ M13 phage carry the linked *hisO* mutation. It should be noted that the level of *hisD* expressed by the His$^-$ *hisO* mutants is essential to this procedure. Since the His$^-$ *hisO* mutations impair expression of *hisD*, only conditional His$^-$ *hisO* mutations have been placed on the M13 phage.

To identify those M13Hol76 phage that contain a *hisO* mutation, we tested for M13 phage that exhibit the phenotype expected of the given *hisO* mutation. For example, to introduce a *hisO* amber mutation onto the phage, M13Hol76*hisD*$^-$ phage grown on this mutant were used to infect a *his* deletion mutant carrying an amber suppressor, selecting Hol$^+$ transductants. Individual transductants were purified and the M13Hol76 phage they release tested for the presence of the *hisO* amber mutation. Mutant (*hisO* amber) M13Hol76 should only transduce to Hol$^+$ a *his* deletion mutant carrying an amber suppressor; wild type (*hisO*$^+$) should transduce recipients carrying no suppressor to Hol$^+$. All of the *hisO* mutations that were crossed onto M13Hol76 have some type of conditional phenotype (amber, ochre, UGA, heat or cold-sensitive), and were verified to be present on the phage by demonstrating that M13Hol76 acquired the expected conditional *hisD* phenotype. Mutations causing a His$^+$ but amino-triazole-sensitive (AT^S) phenotype were verified to be on M13Hol76 by genetic mapping: M13 phage containing an AT^S mutation did not recombine with the same mutation in the chromosome, but did give amino-triazole-resistant recombinants with other mutations not located at the same site.

Revertants (*hisD*$^+$) of M13Hol76 carrying the ochre mutation *hisO9654* were selected by using this phage to transduce a *his* deletion strain (without an ochre suppressor) to Hol$^+$.

The strains carrying the M13Hol76 replicative form DNA that contain the sequenced *hisO* mutations are TT5443 through TT5468, inclusive. Their general genotype is *his-644 zee-1*::Tn*10 leu-414* /F′*pro*$^+$ *lac*$^+$/M13Hol76*hisO*$^-$. (The chromosomes of some of these strains carry *his-9709 hisT1504 pyrB64 metA53*.) The strains that carry nonsense *hisO* mutations on the M13Hol76 DNA also carry the appropriate nonsense suppressors (*supC*, *supF*, or *supI*$^+$).

(b) *Preparation of DNA for sequencing*

(i) *Preparation of single-stranded template*

M13Hol76 DNA was prepared by a modification of the method of Barnes (1978*b*; and personal communication). An M13Hol76-containing strain (strains TT5443 to TT5468, see Table 1) was grown to stationary phase in 200 ml of minimal medium containing 2 mM-histidinol. Cells were removed by centrifugation and the supernatant brought to 0·5 M-NaCl, 2% polyethylene glycol and incubated overnight at 4°C to precipitate the M13Hol76 phage (Yamamoto *et al.*, 1970). The phage precipitate was centrifuged and resuspended in 2·5 ml 100 mM-Tris (pH 7·9), 300 mM-NaCl. Proteinase K (Boehringer Mannheim, 0·25 mg) was added and incubated at 37°C for 1 h. The solution was then deproteinized with 3 vol. water-saturated phenol, followed by 2 extractions with a chloroform/isoamyl alcohol (24:1, v/v) mixture. The DNA was precipitated twice with 300 mM-ammonium acetate and 3 vol. ethanol at −20°C overnight, collected by centrifugation, and resuspended in DNA buffer (10 mM-Tris (pH 7·9), 10 mM-NaCl, 0·1 mM-EDTA) to a final concentration of 1 mg/ml. This procedure routinely yielded 15 to 200 μg of DNA.

(ii) *Preparation of restriction fragments*

Plasmid DNA pWB91 (Barnes, 1977) was purified from a cleared lysate (Katz *et al.*, 1973) using 2 successive CsCl/ethidium bromide gradients by the method of Barnes (1978*a*; and personal communication). This DNA was cut with restriction enzyme *Hin*cII and the resulting fragments were separated by electrophoresis on a 5% to 20% acrylamide gradient gel (Jeppesen, 1974). The fragment bands, visualized under long-wave u.v. light after ethidium bromide staining (0·5 μg/ml), were excised, placed in a 5 ml syringe (plugged with siliconized glass wool), crushed to a fine paste, and soaked overnight at 37°C in 5 ml 500 mM-

ammonium acetate 10 mM-magnesium acetate, 1 mM-EDTA, 0·1% sodium dodecyl sulfate (Maxam & Gilbert, 1977). The solution was collected from the syringe by centrifugation and the DNA precipitated twice with ethanol and resuspended in DNA buffer to a final concentration of 1 mg equivalent/ml. To make smaller fragments suitable for DNA sequencing, fragment R5, which contains all of the *his* control region (Barnes, personal communication), was recut with *Hha*I and the above procedure repeated. All enzymes, unless otherwise noted, were obtained from New England Biolabs, Inc.

(c) *DNA sequencing*

DNA sequencing was done using the dideoxynucleotide chain termination method of Sanger *et al.* (1977) according to Barnes (1978*b*). All *hisO* mutations were sequenced using the restriction fragment RH51 as primer (see Barnes, 1978*b*, for restriction map).

(d) *Enzyme assays*

The *hisD* enzyme, histidinol dehydrogenase, was assayed according to the method of Ciesla *et al.* (1975), as modified by Tadahiko Kohno (personal communication). The reaction contained, per assay, 10 μl 0·1 M-NAD (pH 6·0), 10 μl 0·5 M-glycine (pH 9·8), 10 μl 5 mM-$MnCl_2$, 20 μl [^{14}C]histidinol (approx. 40,000 cts/min), and 50 μl toluenized cells. The reaction was stopped after 1 h by the addition of 0·9 ml 0·05 M-sodium citrate (pH 3·25), and loaded onto a 2-cm Dowex 50X8 column. The [^{14}C]histidine was eluted with 3 ml 0·5 M-sodium citrate (pH 6·0). Specific activity is cts/min per hour per $O.D._{650\,nm}$ unit of cells. [^{14}C]Histidinol was a generous gift from Tadahiko Kohno. The *hisB* enzyme, histidinol phosphate phosphatase, was assayed according to Martin *et al.* (1971).

(e) *Construction of* hisO *double mutants*

To construct the double mutants carrying one of the mutations causing reduced operon expression along with the attenuator deletion *hisO1242*, we selected recombinants that had undergone a recombination event in or near the *his* control region, and then identified the recombinants that had inherited the 2 desired mutations. The design of these crosses is diagrammed in Fig. 1. To select recombinants in the *his* control region, we constructed *hisO* mutant strains carrying a Tn*10* (tetracycline resistance) insertion near, but not in the operon, upstream of the *hisO* mutation of interest, and a Tn*5* (kanamycin resistance) insertion in the *hisG* gene. These strains (TT3602, TT3603, TT3604) were used as donors in transductional crosses with a *hisO1242*, *hisG* double mutant as recipient (TR3063). By selecting the tetracycline-resistant transductants that are also kanamycin-sensitive, we can select only those transductants that have undergone a recombination event in or near the *his* control region. The 3 major types of recombinants arising from this cross are diagrammed in Fig. 1; recombinant type 2 is the desired one.

If the *hisO1242* mutation suppresses the His$^-$ phenotype caused by the *hisO* mutation, then we can identify the 3 recombinant types using a backcross, diagrammed in Fig. 1(b). The *hisO1242* mutation results in a wrinkled colony morphology, due to the high levels of operon expression it causes (Roth *et al.*, 1966; see also Materials and Methods of accompanying paper (Johnston & Roth, 1980)). Wild-type (*hisO*$^+$) colonies have a smooth morphology. If each recombinant type arising from the cross diagrammed in Fig. 1(a) is used as a recipient in a backcross with transducing phage grown on a His$^-$ *hisO* mutant, the colony morphologies of the His$^+$ transductants should identify each recombinant class. Recombinant type 1 should yield both wrinkled (*hisO*^{c}) and smooth (*hisO*$^+$) transductants. The desired recombinant, type 2, should yield only one class of transductants: they will either be wrinkled, if the double mutant exhibits levels of operon expression characteristic of *hisO1242*; or they will be smooth, if the double mutant has reduced levels of operon expression. Colony morphology effects are fully described by Murray & Hartman (1972).

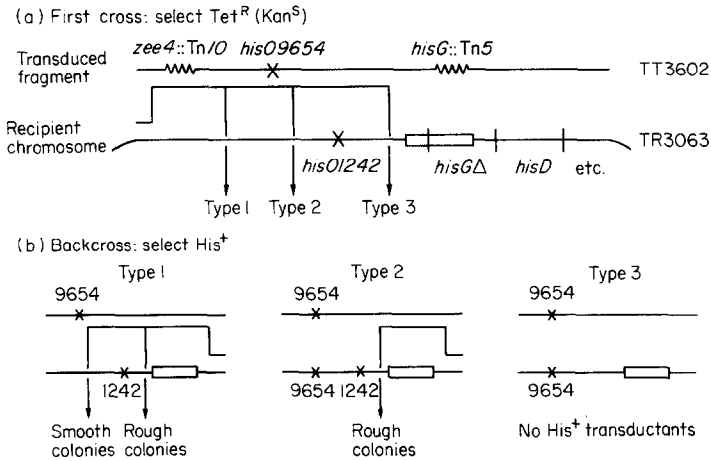

FIG. 1. Crosses to construct *hisO* mutants containing the attenuator deletion *hisO1242*. (a) In the first cross, tetracycline-resistant transductants were picked and scored for absence of Tn*5* (kanamycin sensitivity). For each cross, the following donors gave: TT3602 (*hisO9654*), 116 Kan^S/400 Tet^R; TT3063 (*hisO9663*), 48 Kan^S/100 Tet^R; TT3064 (*hisO9675*), 27 Kan^S/100 Tet^R. (b) In the backcross, His$^+$ was selected, and the colony morphology of the transductants scored. TT3062 as donor yielded 116 Kan^S recombinants in the first cross; 3 gave only rough transductants in the backcross (type 2), 99 gave both rough and smooth transductants (type 1); 3 yielded no His$^+$ transductants in the backcross (type 3). TT3063 as donor yielded 48 Kan^S recombinants in the first cross; 3 were type 2, 45 were type 1. TT3604 as donor yielded 27 Kan^S recombinants in the first cross; 1 was type 2, 26 were type 1.

When double mutants were prepared with *hisO1242* and either the ochre (*hisO9654*) or the UGA (*hisO9675*) mutations, both of which block leader peptide gene translation, or with one of the mutations altering the BC stem (*hisO9663*), one class of recombinants yielded only rough transductants in the backcross (for exact numbers, see the legent to Fig. 1). To verify that this class contains both the *hisO1242* and the *hisO9654*, *hisO9663*, or *hisO9675* mutations (and are therefore type 2 recombinants), the *hisG* deletion was first crossed out of these strains. Both *hisO* mutations were then verified to be present in these strains by the following criteria. (1) They produce wrinkled colonies, and therefore must contain the *hisO1242* mutation. (2) The *hisO9654*, *hisO9663* and *hisO9675* mutations can be separated from the *hisO1242* mutation in these strains and, when separated, cause the same phenotype (His$^-$) as the original mutation. (3) These mutations, when separated from *hisO1242*, map in the correct deletion interval, and are also suppressed by the appropriate suppressors (amber, ochre, UGA). Thus, we feel confident that the class of recombinants that yields only rough transductants in the backcross carry both the *hisO1242* and the *hisO9654*, *hisO9663*, or *hisO9675* mutations.

(f) *Other methods*

All other methods, including cell growth and genetic techniques, have been described (Johnson & Roth, 1979).

(g) *Bacterial and phage strains*

All bacterial strains and their sources are listed in Table 1. Unless otherwise noted, all strains were constructed for this study. Some strains used in this study are listed in Table 1 of Johnston & Roth (1980).

TABLE 1

Multiply marked bacterial strains

Strain	Genotype	Source
TT3136	*hisΔ9708 hisT1505 pyrB64 metA53*/F′*pro*$^+$ *lac*$^+$	
TT3602	*zee-4*::Tn*10 hisO9654 hisG9647*::Tn*5 hisT1504*	
TT3603	*zee-4*::Tn*10 hisO9663 hisG9647*::Tn*5 hisT1505*	
TT3604	*zee-4*::Tn*10 hisO9675 hisG9647*::Tn*5 his T1504*	
TT3670	*hisΔ644 zee-1*::Tn*10*/F′*pro*$^+$ *lac*$^+$	L. Bossi
TT3672	*hisΔ644 zee-1*::Tn*10 leu-414 supF*/F′*pro*$^+$ *lac*$^+$	L. Bossi
TT4415	*hisΔ644 zee-1*::Tn*10 sufJ128*/F′*pro*$^+$ *lac*$^+$/M13Hol76 *hisD3749-S6*	L. Bossi
TT4416	*hisΔ644 zee-1*::Tn*10 supE leu-414*/F′*pro*$^+$ *lac*$^+$/M13Hol76 *hisD6404-C4*	L. Bossi
TT5437	*zee-4*::Tn*10 hisO9663 hisO1242 hisΔOG8439*	
TT5438	*zee-4*::Tn*10 hisO9675 hisO1242 hisΔOG8439*	
TT5439	*zee-4*::Tn*10 hisO9654 hisO1242 hisΔOG8439*	
TT5440	*zee-4*::Tn*10 hisO9663 hisO1242*	
TT5441	*zee-4*::Tn*10 hisO9675 hisO1242*	
TT5442	*zee-4*::Tn*10 hisO9654 hisO1242*	
TT5469	*hisΔ9708 hisT1504 pyrB64 metA53*/F′*pro*$^+$ *lac*$^+$/M13Hol76	
TT5472	*hisΔ644 zee-1*::Tn*10 leu-414 supC zej-636*::Tn*5*/F′*pro*$^+$ *lac*$^+$	
TT5473	*hisΔ644 zee-1*::Tn*10 supU1283*/F′*pro*$^+$ *lac*$^+$	Johnston & Roth (1980)

Unless otherwise noted, all strains were constructed for this study. The nomenclature for Tn*10* insertions has been described (Chumley *et al.*, 1979).

3. The Model for *his* Operon Regulation

Transcription initiating at the *his* promotor produces a leader mRNA that is either terminated at the attenuator site, or is extended through this site to produce *his* structural gene mRNA (Kasai, 1974). The model for *his* operon regulation proposes that the leader transcript can assume one of two conformations by base-pairing to form RNA stem-loop structures. Figure 2 diagrams the *his* leader mRNA sequence, deduced from the *S. typhimurium* DNA sequence (Barnes, 1978*b*), and the two conformations it can assume. Figure 2(a) and (c) show the configuration due to pairing to form one set of stems (AB, CD, and EF): an alternative pairing arrangement of these sequences results in the conformation shown in Figure 2(b) (BC and DE stems). The model proposes that the formation of one of these stems, the EF stem, causes transcription to terminate within the run of nine U residues distal to this stem. Transcription has been shown to terminate at sites similar to this in other systems (see Adhya & Gottesman, 1978, for review). For this reason, the EF stem is termed the attenuator stem. The leader RNA conformation shown in Figure 2(a) and (c) includes the attenuator stem and therefore leads to transcription termination. The configuration shown in Figure 2(b) does not include the attenuator stem and hence would allow transcription to proceed into the *his* structural genes.

Which of the two alternative conformations the *his* leader RNA assumes is determined by the extent of translation of the leader peptide gene. We assume that a ribosome translating this small gene prevents the formation of secondary

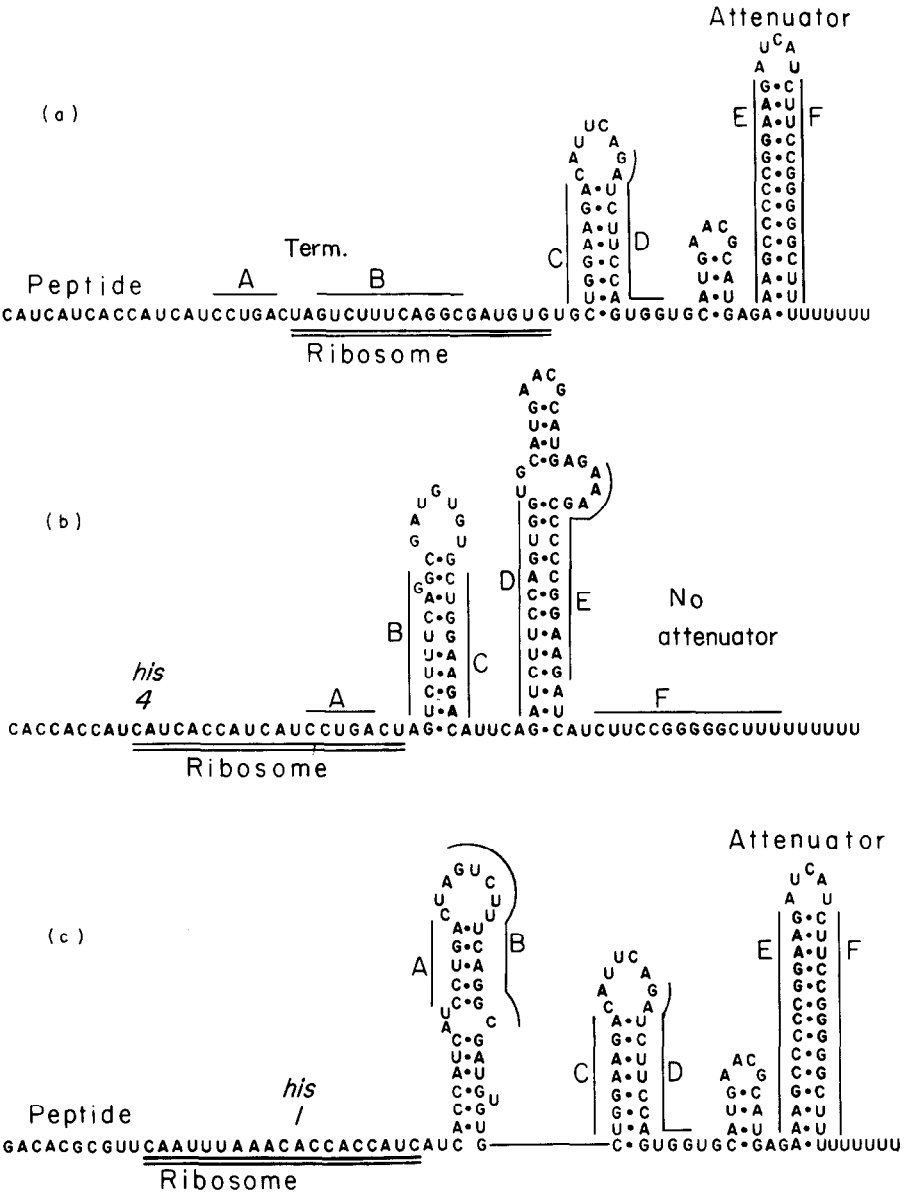

FIG. 2. Alternative secondary structures for the histidine operon leader mRNA. The stems can be drawn in several slightly different ways; the form chosen is predicted to be thermodynamically favored (Borer *et al.*, 1974; Bloomfield *et al.*, 1974). The letters (A to E) denote the stretches of sequence involved in the alternative structures. The length of message presumed to be covered by the translating ribosome is above the double lines. Hyphens have been omitted for clarity.

structure in the 16 ribonucleotides 3′ to the codon occupying the aminoacyl site on the ribosome. The effect of varying the extent of leader peptide gene translation on leader RNA secondary structure is shown in Figure 2. Figure 2(a) presents the situation when the cell is growing with high levels of histidyl-tRNA, which allow

the ribosome to proceed rapidly through the run of seven histidine codons. The ribosome has stopped translation at the UAG terminator codon of the leader peptide gene, and in this position prevents formation of the AB stem. As the polymerase continues transcription, leaving the ribosome behind, the CD stem forms, followed by the attenuator (EF) stem, which causes transcription termination. Figure 2(b) shows the situation when the cell becomes limited for histidyl-tRNA due to histidine starvation. The ribosome is stalled in the run of histidine codons and prevents A sequences from forming stem structures. As the polymerase proceeds, the BC stem can form, followed by the DE stem, which prevents attenuator (EF) stem formation and allows transcription to continue through the attenuator site. Figure 2(c) presents the outcome if the leader peptide gene is not translated, or if the ribosome stalls before the run of *his* codons. A ribosome stopped before the first histidine codon prevents no stem structures from forming. As transcription proceeds, the AB, CD and, finally, the attenuator (EF) stems form, resulting in transcription termination. This sequence of events explains the requirement of *hisO* translation for *his* operon expression *in vitro* (Artz & Broach, 1975).

This model is necessarily a kinetic one, because calculations suggest that the configuration that includes the EF stem is thermodynamically more stable than the alternative conformation. We assume that the relative thermodynamic stabilities will determine which stems are able to form and that, once formed, these stems are stable over the time-scale involved in making the regulatory decision.

In this paper, we present the DNA sequence changes of many of the *hisO* mutations described by Johnston & Roth (1980) (accompanying paper). These alterations are discussed in relation to the above model for *his* operon regulation.

4. Results and Discussion

The *his* operon control region (*hisO*), and the first two *his* structural genes (*hisG* and *hisD*) have been cloned into the single-stranded DNA phage M13 (Barnes, 1979). The hybrid phage provides a convenient source of DNA for determining DNA sequence by the chain-termination method of Sanger *et al.* (1977) and Barnes (1978). To determine the DNA sequence changes of *hisO* mutations, these mutations were placed on the M13-*hisOGD* hybrid phage by normal recombination *in vivo* (see Materials and Methods). Each mutation was verified to be present on the M13-*hisOGD* phage by genetic criteria (see Materials and Methods). Single-stranded DNA was isolated from M13 phages carrying the *hisO* mutation, and used as template to determine the DNA sequence changes of the mutations. Some representative sequencing data are presented in Figure 3.

(a) *Mutations affecting the leader peptide gene*

Three mutations lie in the leader peptide gene: their sequence changes are presented in Figure 4. Two of these mutations (*hisO9654* and *hisO9675*) prevent operon expression (cause a His^- phenotype), and one (*hisO9876*) causes low levels of operon expression that do not increase in response to histidine starvation.

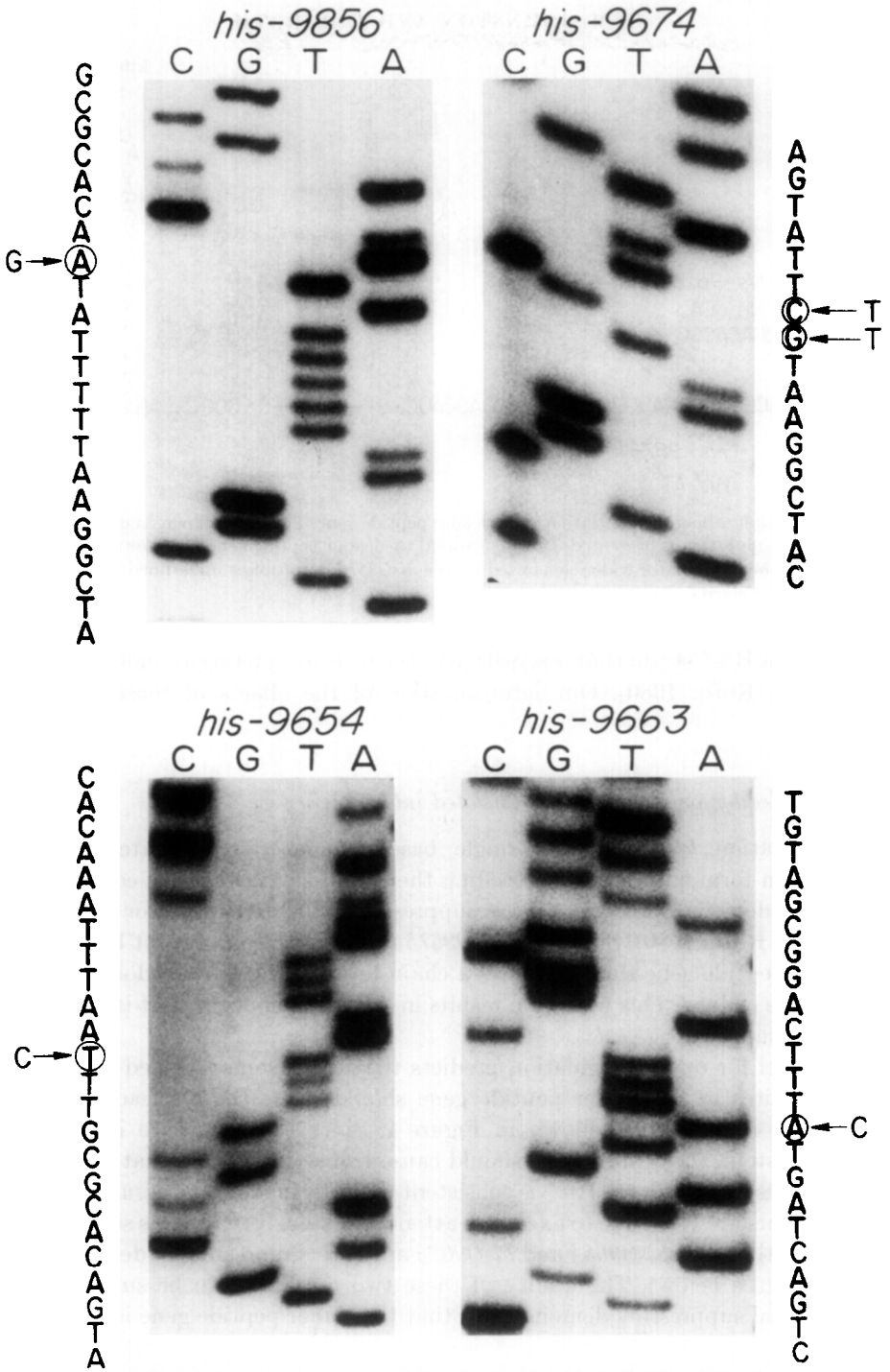

FIG. 3. Representative sequence data of selected *hisO* mutants. The sequence was generated using restriction fragment RH51 as primer (see Barnes, 1978*b*, for restriction map) on M13Hol76 carrying one of the *hisO* mutations as template (see Barnes, 1979, and Materials and Methods). The sequence around each mutation is labelled in the Figure. The mutated bases are circled.

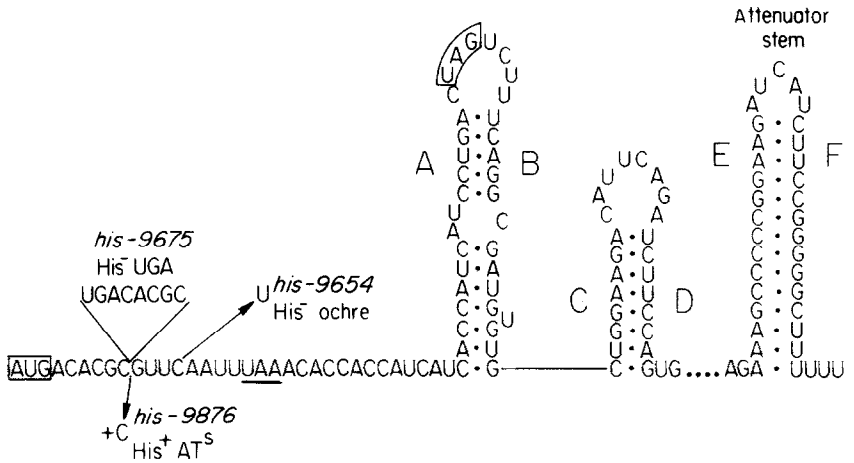

FIG. 4. Mutations affecting translation of the leader peptide gene. The base change, and the phenotype caused by each mutation is presented. Boxes surround the leader peptide gene initiator and terminator codons. The ochre terminator codon generated by the *hisO9876* mutation is underlined. Hyphens have been omitted for clarity.

resulting in a His^+ strain that is sensitive to the histidine analog amino-triazole (see Johnston & Roth, 1980). Our interpretation of the effects of these mutations follows.

(i) *The* his *leader peptide gene is translated into protein*

The mutation *hisO9654* is a single base change that generates an ochre (UAA) chain-terminator codon preceding the run of seven histidine codons in the leader peptide gene. This mutation is suppressed by ochre suppressor tRNAs (see Johnston & Roth, 1980). Similarly, *hisO9675* is a duplication of eight bases within the leader peptide gene that generates a chain-terminating UGA codon in front of the histidine codons. This mutation results in a His^- phenotype that is suppressed by a UGA suppressor (*supU*).

The model for operon regulation predicts that a ribosome stopped at either of these two sites in the leader peptide gene should cause the *his* leader RNA to assume the conformation shown in Figure 4. Since this structure includes the attenuator stem, these mutations should cause transcription termination, and the fact that these mutants are His^- is consistent with the model. The assumption that these mutants are His^- due to excessive attenuator stem formation is supported by the observation that *hisO9654* and *hisO9675* are both suppressed by deletion of the attenuator (see below). The ability of these two mutations to be suppressed by informational suppressors demonstrates that the leader peptide gene is translated.

(ii) *The extent of leader peptide gene translation is central to regulation*

The *hisO9654* and *hisO9675* mutations cause ribosomes to stop nine and 20 bases, respectively, in front of the first histidine codon of the leader peptide gene. A

ribosome halted at these sites results in a His^- phenotype, presumably due to excessive attenuator stem formation. In contrast, the +1 frameshift mutation, *hisO9876*, causes the ribosome to terminate at an ochre (UAA) codon only four bases before the first histidine codon. This mutation causes a His^+ AT^S phenotype that is suppressed by ochre suppressors. Apparently, a ribosome stopped this close to the run of histidine codons prevents attenuator stem formation often enough to result in a His^+ phenotype, while a ribosome halted at the other two positions is never able to prevent attenuator stem formation (causing a His^- phenotype). This result can be explained if we assume that 16 to 20 ribonucleotides 3′ to the aminoacyl site on the ribosome are unable to participate in stem-loop structures. This is slightly larger than the length of RNA protected from nuclease digestion by translating ribosomes (Steitz, 1979). However, it is conceivable that the ribosome could disrupt a larger length of RNA secondary structure than it is able to protect from nuclease digestion. A ribosome covering 16 to 20 bases would be unable to disrupt the AB stem when stopped at the *hisO9654* or *hisO9675* sites; this would result in excessive attenuator stem formation. However, a ribosome stopped at the ochre codon generated by *hisO9876* might cause frequent disruption of the AB stem located 14 nucleotides downstream of this ochre codon. This would lower the frequency of attenuator stem formation by allowing the BC and DE stems to form occasionally (Fig. 2(b)) and permit transcription to proceed through the attenuator site. In fact, there is a direct correlation between the distance the ribosome advances in the leader peptide gene, and the level of operon expression: the *hisO9876* mutation causes a His^+ phenotype, the *hisO9654* mutant is leaky His^-, and *hisO9675* is a tight His^- mutant. The levels of operon expression in these mutants, presented as *hisD* enzyme levels, are shown in Table 2. These results suggest that the extent of ribosome advance in the leader peptide gene is central to the regulatory mechanism.

TABLE 2

Histidinol dehydrogenase levels in leader peptide gene mutants

Strain	*hisO* mutation	Relative spec. act.	No. of bases from nonsense codon to base of AB stem
LT2	Wild type	1·0	
TR5758	*hisO9876*	1·4	14
TR5580	*hisO9654*	0·6	19
TR5601	*hisO9675*	0·2	30

Cells grown to late log phase ($O.D._{650} \sim 1·0$) in 0·8% nutrient broth +0·5% NaCl were assayed as described in Materials and Methods. Specific activity is the amount of [^{14}C]histidinol converted to [^{14}C]histidine (cts/min) per ml of cells per hour per $O.D._{650}$ unit of cells. The specific activity of LT2 was $1·3 \times 10^5$.

(iii) *The leader peptide has no function*

The *hisO* mutations, including those that lie in the leader peptide gene, are *cis*-dominant. Therefore, either the leader peptide gene produces a non-functional

product, or its product is a *cis*-acting protein. Consistent with the first possibility is the fact that all three of the leader peptide gene mutations are nonsense or frameshift mutations. The properties of two of the leader peptide gene mutants, discussed below, support the first possibility.

The *hisO9675* mutation, in addition to generating a UGA codon, causes a shift to the −1 reading frame of the leader peptide gene due to the duplication of eight bases. Therefore, when this mutation is suppressed by a UGA suppressor, it causes the production of a leader peptide substantially different from the wild-type peptide. Nonetheless, the suppressed UGA mutant (*hisO9675*) has a His^+ phenotype. Similarly, the +1 frameshift mutant (*hisO9876*) is His^+, even though it produces a shortened peptide. These results imply that the leader peptide is not required for at least some transcription to proceed through the attenuator site. Instead, it is probably only the act of translation of the leader peptide that is responsible for readthrough of the attenuator site by RNA polymerase. It is possible, although we believe unlikely, that the leader peptide is required to obtain fully derepressed levels of operon expression.

(iv) *Reduced leader peptide gene translation causes reduced operon expression*

As diagrammed in Figure 2(c), less translation of the leader peptide gene should result in reduced operon expression due to the increased frequency of attenuator stem formation. Five mutational changes, diagrammed in Figure 5, presumably impair initiation of translation of the leader peptide gene. Three of these changes affect the AUG initiator codon of the leader peptide gene; the other two alter sequences just in front of the initiator codon. The effects of these mutations on operon regulation are discussed below.

The mutations *hisO9709*, *hisO9613*, *hisO9856*, *hisO9866* and *hisO9867* presumably reduce the efficiency of translation initiation of the leader peptide

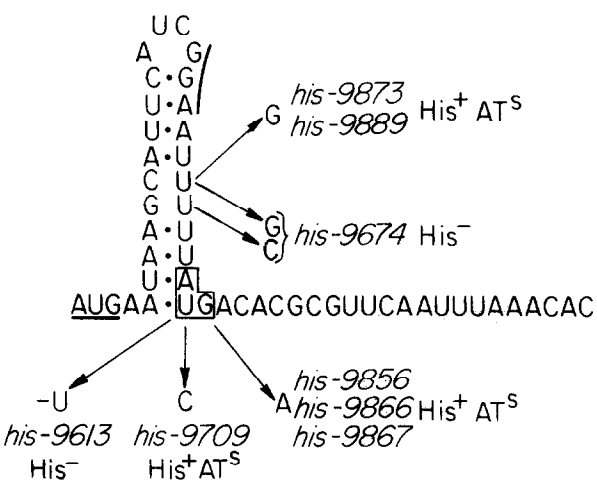

FIG. 5. Mutations affecting leader peptide gene translation initiation. The sequence complementary to the 3′ end of 16 S rRNA (GGA) is underlined. Also underlined is an AUG codon that is in the −1 reading frame of the leader peptide gene. The leader peptide gene initiator codon is enclosed in the box. Hyphens have been omitted for clarity.

gene, since they change the AUG initiator codon. The fact that these mutants exhibit reduced operon expression is consistent with the model for operon regulation. An analogous mutation in the *trp* operon leader peptide gene has a similar phenotype (Zurawski *et al.*, 1978*b*). The model for operon regulation predicts that the absence of translation of the leader peptide gene should cause exclusive attenuator stem formation, and the His^- phenotype of the *hisO9654* (ochre) and *hisO9675* (UGA) mutants confirms this prediction. The *hisO9613* mutation results in a His^- phenotype, presumably by preventing any initiation of leader peptide gene translation. The fact that *hisO9709*, *hisO9856*, *hisO9866* and *hisO9867* are His^+ suggests that there must be some low-level translation of the leader peptide gene in these mutants. We propose two explanations for how this could occur. First, the ACG and AUA codons in these mutants might provide low-level initiation of leader peptide gene translation. A mutant T4 AUA codon is able to serve as an initiator for translation (Belin *et al.*, 1979; Belin, 1979). A mutant T7 phage gene whose initiator codon is changed to ACG produces a low but detectable level of protein, but in this case it is not clear if the ACG codon is serving as the initiator (Dunn *et al.*, 1978). Second, it is possible that ribosomes in these mutants are using a different AUG codon to initiate leader peptide gene translation. The AUG codon that precedes the leader peptide gene by 26 nucleotides (underlined in Fig. 4), could serve to initiate translation. Translation beginning from this site is out of frame with respect to the leader peptide gene and would normally terminate at the UGA codon beginning with the second nucleotide of the leader peptide gene. The *hisO9709* mutation changes this codon to CGA and would allow translation to proceed well past the end of the leader peptide gene (to a UGA codon 101 nucleotides downstream from the leader peptide gene initiator). However, the *hisO9856*, *hisO9866* and *hisO9867* mutations generate an ochre (UAA) chain-terminator codon at this position, in frame with the alternative AUG initiator codon. Therefore, ribosomes initiating at this alternative AUG cannot be expected to permit leader peptide gene translation in these mutants. Since there is no other AUG (or GUG) codon that could serve to initiate leader peptide gene translation (Barnes, personal communication), it is probable that translation initiates at the AUA codon in mutants *hisO9856*, *hisO9866* and *hisO9867*.

Furthermore, it seems unlikely that the alternative AUG codon is used to initiate translation in the *hisO9709* (ACG) mutant. The *hisO9613* mutation alters the UGA codon that is in phase with the alternative AUG initiator, and would allow ribosomes initiating from this site to proceed to an ochre (UAA) codon four nucleotides in front of the first histidine codon of the leader peptide gene. We know from the phenotype of the *hisO9876* mutant (discussed above) that ribosomes proceeding to this point cause a His^+ AT^S phenotype. The fact that the *hisO9613* mutant is His^- suggests that translation does not initiate from the alternative AUG codon.

Two other mutational changes affect nucleotides just in front of the leader peptide gene initiator codon, and presumably reduce translation initiation by altering the ribosome binding site. One pair of mutations (*hisO9873* and *hisO9889*) result in low levels of operon expression (His^+ AT^S phenotype); the other mutation (*hisO9674*) completely blocks operon expression (His^- phenotype). Since neither of

these mutations directly affect the sequence complementary to the 3′ and of 16 S rRNA (Shine & Dalgarno, 1974), it is not immediately clear how they could affect ribosome binding. Examination of the surrounding sequence suggests a possible mechanism. In wild type, a stem-loop structure in the leader RNA can be drawn in this region (Fig. 5). This stem includes two of the three nucleotides complementary to the 3′ end of 16 S rRNA (GGA), and the first two bases of the AUG initiator codon. These sites, if paired in such a stem, might not be available to bind ribosomes. Since this stem-loop structure is relatively unstable in wild type (see Table 3), it may not form significantly and should have little effect on ribosome binding. However, in the mutants, this stem is much more stable, and could cause a reduction of translation initiations. There is a direct correlation between the strength of this stem in the mutants and the level of operon expression (Table 3). Models similar to this have been suggested to explain reduced translation initiation in mutants of phage f2 (Atkins *et al.*, 1979), and in phage lambda (Iserentenant & Fiers, 1980).

TABLE 3

Thermodynamic stabilities of initiator stem-loop structure

Mutation	ΔG of stem	Phenotype
Wild type	−3·0	His^+ AT^R
his9873	−7·2	His^+ AT^S
his9889		
his9674	−14·4	His^-

Calculated stabilities (ΔG) of a stem-loop structure including the leader peptide gene initiator region. The ΔG values of the stem were calculated according to Bloomfield *et al.* (1974). Also noted are the phenotypes caused by the 2 mutation types.

(b) *Mutations altering the RNA stem-loop structures*

Nineteen *hisO* mutations probably affect the stability of the leader mRNA stem-loop structures that prevent formation of the attenuator stem (Fig. 2(b)). Some of them prevent operon expression (causing a His^- phenotype) and some of them cause only reduced levels of operon expression (His^+ AT^S phenotype). Their sequence changes are presented in Figure 6 and are discussed below.

(i) *All mutations weaken one set of alternative stems*

All mutations are predicted to reduce the stability of one of the two stems (BC and DE) that are alternatives to the attenuator (EF) stem. Presumably, the BC and DE stems form less frequently because of these mutations, resulting in excessive formation of the attenuator stem. The calculated stabilities of each of the stems for wild type, and for each mutant are presented in Table 4. In general, the mutations causing the greatest reduction in BC or DE stem stabilities result in a His^- phenotype. Apparently the BC and DE stems never form in these mutants,

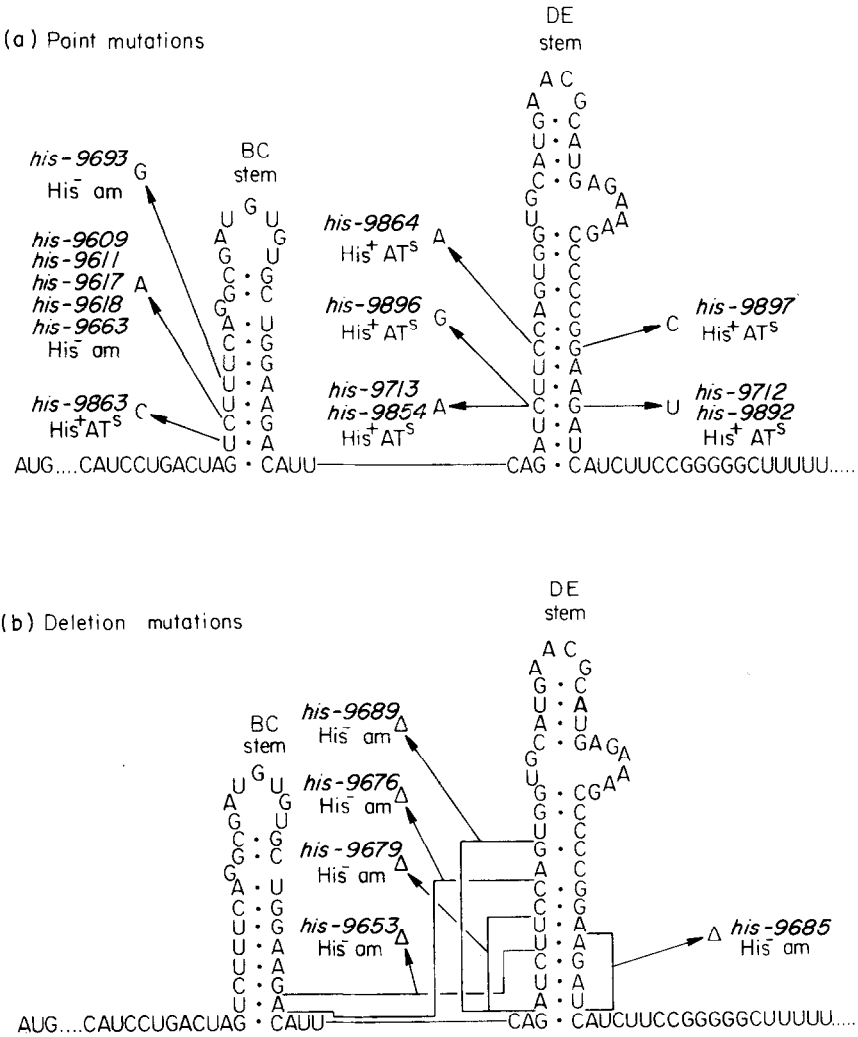

FIG. 6. Mutations affecting the mRNA stem-loop structures. The base changes and the phenotype caused by each mutation is presented. The first codon in the Figure is the leader peptide gene initiator codon. Hyphens have been omitted for clarity.

resulting in exclusive attenuator stem formation, thus preventing operon expression. This is supported by the fact that a deletion of the attenuator stem serves to suppress one of these mutants (*hisO9663*, see below). Seven mutations that cause the least reduction in the stability of the DE stem (*hisO9712*, *hisO9713*, *hisO9854*, *hisO9864*, *hisO9892*, *hisO9896* and *hisO9897*) result in a His^+ AT^S phenotype. One mutation (*hisO9863*) that reduces the stability of the BC stem also causes a His^+ AT^S phenotype. Presumably, the BC and DE stems are able to form in these mutants at some low frequency, occasionally preventing attenuator stem formation and allowing transcription to proceed into the structural genes. The sequence changes and phenotypes of these mutants are consistent with a role for

TABLE 4

Calculated thermodynamic stabilities of his *leader mRNA stem-loop structures*

Mutation	Stems AB	BC	CD	DE	EF	Phenotype
Wild type	−16·2	−10·2	−11·2	−18·0	−38·4	His^+ AT^R
hisO9653		−5·8	−4·4	−9·6		His^-
hisO9663		−3·8				His^-
hisO9679			−3·4	−6·2		His^-
hisO9685				−8·4	−35·2	His^-
hisO9689			>0	−3·2		His^-
hisO9693		−7·0				His^-
hisO9712				−11·6	−36·2	His^+ AT^S
hisO9713			−4·8	−11·6		His^+ AT^S
hisO9863		−3·8				His^+ AT^S
hisO9864			−2·0	−8·8		His^+ AT^S
hisO9897				−8·8	−29·2	His^+ AT^S
hisO9922					−30·4	(see text)

Calculated stabilities (ΔG) of histidine operon leader mRNA stem-loop structures. The calculated free energies of formation (ΔG, in kcal/mol, Borer *et al.*, 1974; Bloomfield *et al.*, 1974) of each stem-loop structure are presented. The phenotype caused by each mutation is also noted.

the BC and DE stems in preventing attenuator stem formation.

Four mutations (*hisO9712*, *hisO9685*, *hisO9892* and *hisO9897*) reduce the stability of both the DE and the attenuator (EF) stems (Table 4). Since these mutations cause reduced operon expression, we believe that the relatively minor changes near the top of the attenuator stem do not appreciably impair its ability to form and cause transcription termination.

(ii) *Amber suppressor tRNAs suppress BC and DE stem mutants*

Genetic characterization of the His^- *hisO* mutants revealed that many of them are suppressed by amber suppressors (see Johnston & Roth, 1980). Unlike the ochre and UGA mutations, the amber-suppressible mutations do not generate nonsense codons in the leader peptide gene (no codon in this gene can be converted to UAG by a single base change). We discovered that all of the His^- mutations that weaken the BC or DE stems are suppressed by amber suppressors, even though none of them generate an amber codon, nor do they even lie in a region of *hisO* thought to be translated.

We believe that suppression of these mutations by amber suppressor tRNAs is due to ribosomes that read through the normal terminator codon (UAG) of the leader peptide gene. A ribosome allowed to read through this terminator codon would proceed to a UGA codon at the base of the attenuator stem (five nucleotides in front of the base of the EF stem). A ribosome following polymerase closely up to this point would prevent attenuator stem formation and allow transcription to proceed through the attenuator site. Since very little operon expression is required for a His^+ phenotype (about 0·1 of basal levels), relatively few ribosomes would

need to read through the leader peptide gene terminator to elicit suppression. The fact that all of the His$^-$ stem mutants are suppressed by amber suppressors, even though they all result in different sequence changes, is consistent with this model for the mechanism of suppression.

This explanation for suppression of these mutations predicts that amber suppressors should cause increased operon expression in wild-type cells. In fact, strains wild-type for *hisO* containing various amber or ochre suppressors (both of which are able to read UAG) have two- to threefold increased levels of *his* operon expression (Johnston *et al.*, 1980; Chumley, 1980).

(iii) *Only the EF stem is responsible for attenuation*

The model proposes that the EF (attenuator) stem is responsible for the termination of transcription at the attenuator site. However, since both of the leader RNA structures that include the attenuator stem also include the CD stem (Fig. 2(a) and (c)), it is possible that CD is also required for transcription termination. The four mutations that delete D sequences (*hisO9653*, *hisO9676*, *hisO9679* and *hisO9689*) rule out this possibility. None of these mutants should be able to form the CD stem, yet they are all His$^-$, presumably due to excessive attenuator stem formation. Therefore, transcription termination is complete even in the absence of the CD stem. The role of the CD stem, then, must simply be to sequester D sequences, thus preventing DE stem formation, and allowing formation of the attenuator (EF) stem.

(c) *Mutations altering the attenuator stem*

The DNA sequence changes of two mutations that alter the attenuator stem are presented in Figure 7. One of these mutations, *hisO1242*, was sequenced by Wayne Barnes and has been described (Johnston *et al.*, 1980). It is discussed here in relation to the other *hisO* mutations, and in the context of the model for *his* operon regulation. The other attenuator mutation, *hisO9922*, is a new mutation isolated in this study. These mutations are discussed below.

(i) *The attenuator stem causes transcription termination*

The *hisO1242* mutation causes constitutively high levels of operon expression (Roth *et al.*, 1966), and prevents transcription termination at the attenuator site (Kasai, 1974). The fact that this mutation deletes E and F sequences, and thus prevents formation of the attenuator stem strongly suggests that this stem is responsible for the termination of transcription (Barnes, 1978*b*). The observation that *hisO1242* suppresses mutants that are His$^-$ presumably due to excessive attenuator stem formation strengthens this conclusion (see below).

(ii) *Revertants of* hisO *mutants have attenuator stem lesions*

All of the His$^-$ mutations that map between the *his* promotor and the attenuator, including those described here, revert to His$^+$ at a very high

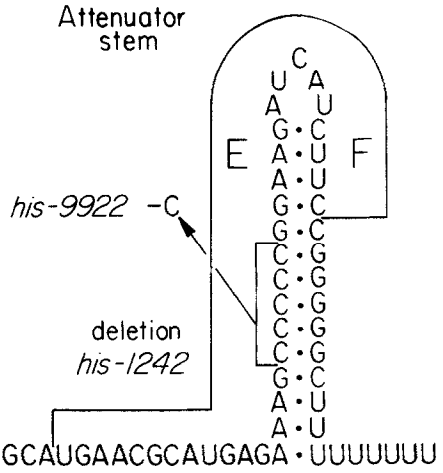

FIG. 7. DNA sequence changes of 2 mutations that alter the *his* attenuator stem. Refer to the text for a discussion of these 2 mutations. Hyphens have been omitted for clarity.

spontaneous frequency (10^{-5} to 10^{-6}); this frequency is increased by both base substitution and frameshift inducing mutagens (see Johnston & Roth, 1980). This suggests that the *hisO* mutations are being suppressed by second-site mutations in these revertants, as was shown to be the case by Johnston & Roth (1980). The model for operon regulation explains these reversion properties, and predicts the sequence changes of some of the second-site suppressor mutations.

According to the model, all of the His^- mutants defective in leader peptide gene translation or in alternative stem formation are unable to express the operon due to excessive formation of the attenuator stem. Any mutation that reduces the stability or frequency of formation of the attenuator stem should therefore suppress these mutations. The large number of ways of impairing the attenuator stem or its formation could explain the high reversion frequency of these mutations.

The ochre mutation *hisO9654*, when present on the M13-*hisOGD* hybrid phage, prevents expression of the *hisG* and *hisD* genes present on this phage. We isolated a revertant phage able to express the *hisD* gene (see Materials and Methods), and sequenced the second-site suppressor mutation. As shown in Figure 7, the new mutation (*hisO9922*) is a deletion of one base from the attenuator stem, which apparently destabilizes the attenuator stem sufficiently (about 8 kcal, see Table 4) to allow some operon expression. That such a minor destabilization of the attenuator stem allows operon expression is consistent with the fact that only low levels of expression are required for the $hisD^+$ phenotype. However, since the M13-*hisOGD* hybrid phage replicative form may exist in the cell in many copies (Hohn *et al.*, 1971; Barnes, 1979), such minor attenuator stem defects could cause the $hisD^+$ phenotype when present on the phage, but not when present in the chromosome. Nevertheless, this result suggests that many revertants of the His^- *hisO* mutants carry mutations altering the attenuator stem, and further indicates that the attenuator stem is responsible for transcription termination.

(d) *Deletion of the attenuator stem suppresses* hisO *mutations*

We have argued that the *hisO* mutations that alter the RNA stem-loop structures or affect leader peptide gene translation cause reduced operon expression due to excessive attenuator stem formation. If this is correct, then these mutations should be suppressed by deletion of attenuator stem sequences. We have constructed double mutants carrying the attenuator deletion *hisO1242* and one of three mutations (*hisO9663*, *hisO9654*, *hisO9675*) affecting leader peptide gene translation or alternative stem formation. The fact that these double mutants have the wrinkled colony morphology characteristic of *hisO1242* indicates that their levels of operon expression are similar to that in a *hisO1242* mutant. This is demonstrated by measurement of *hisB* enzyme levels in these strains, presented in Table 5. Therefore, the *hisO* mutants that are His^- due to excessive attenuator stem formation are completely suppressed by deletion of the attenuator. The construction of these double mutants is described in Materials and Methods.

5. Further Discussion

Under conditions of excess histidine availability, the *his* operon is still expressed at a substantial basal level. Since the His^- *hisO* mutants owe their phenotype to excessive formation of the attenuator stem, this stem is able to block virtually all transcription. Therefore, the basal levels of expression cannot be due to the inability of the attenuator stem to prevent readthrough. Instead, the basal levels must reflect the frequency with which the attenuator stem does not form under repressed conditions, caused by formation of the alternative set of stems (BC and DE, Fig. 2(b)). This could be due to statistical fluctuations in ribosome position under fully repressed conditions. If occasionally the first ribosome is slowed due to transient decreases in concentration of any of the charged tRNAs, or is late in initiating leader peptide gene synthesis, the attenuator stem would not form. The RNA stem-loop structure that includes the initiator region of the leader peptide gene (Fig. 5) could be responsible for setting the basal level of operon expression. If this stem occasionally forms under repressing conditions, it would cause some ribosomes to be late in initiating leader peptide gene synthesis, resulting in occasional disruption of the attenuator stem. Another possible mechanism could involve release of the ribosome from the leader mRNA. A ribosome halted at the terminator codon of the leader peptide gene could slightly disrupt the CD stem, situated 19 nucleotides downstream from the terminator codon. If the ribosome remained at this position while the polymerase synthesized E stem sequences, the DE stem would form, preventing attenuator stem formation. However, if the ribosome was released from the leader mRNA while polymerase was synthesizing D stem sequences, the CD stem would form, allowing formation of the attenuator stem. Thus, the basal levels could reflect random differences in the time of ribosome release at the leader peptide gene terminator codon.

Many of the *hisO* mutations result in a temperature-dependent phenotype: some *hisO* mutants are heat-sensitive, and some are cold-sensitive (see Johnston & Roth, 1980). Although the basis for these effects is not clear, they may reflect the effects

of temperature on mRNA secondary structure. All the point mutations, and one deletion mutation (*hisO9653*) affecting the BC and DE stems are heat-sensitive. This could be due to the possibility that the stabilities of these stems, which are already reduced by the mutations, are further reduced at high temperatures, leading to more frequent attenuator stem formation. The ochre mutant *hisO9654* is cold-sensitive. This might be due to less frequent attenuator stem formation due to the decreased stabilities of this stem at high temperatures. The interpretation of the temperature effects is complicated, however, since temperature could effect many different functions, including translation and transcription rates, frequency of translation initiations, and translation and transcription termination.

All of the mutations affecting the alternative stems BC and DE are suppressed by amber suppressors. However, the mutations altering the BC stem seem to be more strongly suppressed than those affecting the DE stem (see Table 5 of Johnston & Roth, 1980): BC stem mutants are suppressed well in a *hisT*$^-$ strain: the DE mutants are suppressed weakly in *hisT*$^-$ strains. Both BC and DE stem mutants are more strongly suppressed in *hisT*$^+$ strains. Reasons for the *hisT* effect on suppression are not clear. The explanation of suppression that we favor is that the suppressor causes ribosomes to read through the terminator codon (UAG) of the leader peptide gene. These ribosomes follow polymerase closely and ultimately disrupt the attenuator stem (see Results, section (b)). In *hisT* mutants, ribosomes are thought to move more slowly (especially through the run of *his* codons) due to their lack of anticodon loop pseudouridine residues (Johnston *et al.*, 1980). We suggest that when ribosomes are thus delayed they do not follow RNA polymerase closely enough to adequately disrupt the attenuator stem. It is not clear why the DE stem mutations are suppressed less strongly than the BC stem mutations.

It is interesting to note that all of the mutations that disrupt the alternative stems BC and DE alter the bottom part of each stem (see Fig. 6). Apparently, mutations in the upper part of these stems have little or no affect on operon expression. In fact, it is only the upper part of the BC and DE stems that contain unpaired sequences. This suggests that only the bottom halves of these stems are critical to the regulatory mechanism.

Unlike the *trp* operon, histidine specific regulation of the *his* operon appears to occur entirely at the level of transcription termination at the attenuator site: the initiation of transcription at the promotor is not specifically regulated by histidine levels. This conclusion is drawn from the fact that, in the *hisO1242* mutant, operon expression does not increase appreciably in response to histidine starvation (Roth *et al.*, 1966). General metabolic regulation of the operon however, which is sensitive to guanosine tetraphosphate levels, is presumably mediated at the promotor (Stephens *et al.*, 1975: Winkler *et al.*, 1978).

The genetic map of the *his* control region contains a number of mutations that map near the attenuator and cause constitutive high levels of operon expression (Ely *et al.*, 1974: see Johnston & Roth, 1980). We believe that all of these mutations, like *hisO1242*, will affect the stability or formation of the attenuator stem. The constitutive mutations that map under *hisO1242* almost certainly affect E or F sequences. The mutations that map just upstream of *hisO1242* might affect C sequences, thus preventing CD stem formation and causing excessive formation

of the DE stem. Both types of mutations would be expected to form the attenuator stem less frequently and lead to high levels of operon expression. Such C sequence mutations probably account for the interspersion in the *hisO* genetic map of constitutive mutations and mutations causing reduced operon expression.

We are extremely grateful to Wayne Barnes for teaching one of us (H.M.J.) DNA sequencing techniques, for communicating unpublished information, and for providing the M13Hol76 phage prior to publication. Without his generous help, this paper would not have been possible. We also thank Lionello Bossi, for collaborating on the M13 genetics, and Tadahiko Kohno, for his generous gift of [^{14}C]histidinol. This work was supported by National Institutes of Health grant GM23408.

REFERENCES

Adhya, S. & Gottesman, M. (1978). *Annu. Rev. Biochem.* **47**, 967–996.
Artz, S. W. & Broach, J. R. (1975). *Proc. Nat. Acad. Sci., U.S.A.* **72**, 3453–3457.
Atkins, J. F., Steitz, J. A., Anderson, C. W. & Model, P. (1979). *Cell*, **18**, 247–256.
Barnes, W. M. (1977). *Science*, **195**, 393–394.
Barnes, W. M. (1978*a*). *J. Mol. Biol.* **119**, 83–99.
Barnes, W. M. (1978*b*). *Proc. Nat. Acad. Sci., U.S.A.* **75**, 4281–4285.
Barnes, W. M. (1979). *Gene*, **5**, 127–139.
Belin, D. (1979). *Mol. Gen. Genet.* **171**, 35–42.
Belin, D., Hedgpeth, J., Selzer, G. B. & Epstein, R. H. (1979). *Proc. Nat. Acad. Sci., U.S.A.* **76**, 700–704.
Bertrand, K., Korn, L., Lee, F., Platt, T., Squires, C. L., Squires, C. & Yanofsky, C. (1975). *Science*, **189**, 22–26.
Bloomfield, V., Crothers, D. & Tinoco, I. Jr (1974). In *Physical Chemistry of Nucleic Acids*, pp. 343–353, Harper and Row, New York.
Borer, P., Dengler, B., Tinoco, I. Jr & Uhlenbeck, O. (1974). *J. Mol. Biol.* **86**, 843–853.
Bossi, L. & Roth, J. R. (1980). *Nature (London)*, **286**, 123–127.
Chumley, F. G. (1980), Ph.D. dissertation, University of California, Berkeley.
Chumley, F. G., Menzel, R. & Roth, J. R. (1979). *Genetics*, **91**, 639–655.
Ciesla, Z., Salvatore, F., Broach, J. R., Artz, S. W. & Ames, B. N. (1975). *Anal. Biochem.* **62**, 44–55.
DiNocera, P. P., Blasi, F., DiLauro, R., Frunzio, R. & Bruni, C. B. (1978). *Proc. Nat. Acad. Sci., U.S.A.* **75**, 4276–4280.
Dunn, J. J., Buzash-Pollert, E. & Studier, F. W. (1978). *Proc. Nat. Acad. Sci., U.S.A.* **75**, 2741–2745.
Ely, B., Fankhauser, D. B. & Hartman, P. E. (1974). *Genetics*, **78**, 607–631.
Gardiner, J. (1979). *Proc. Nat. Acad. Sci., U.S.A.* **76**, 1706–1710.
Gemmill, R. M., Wessler, S. R., Keller, E. B. & Calvo, J. M. (1979). *Proc. Nat. Acad. Sci., U.S.A.* **76**, 4941–4945.
Hohn, B., Lechnerl, H. & Marvin, D. A. (1971). *J. Mol. Biol.* **56**, 143–156.
Iserentenant, D. & Fiers, W. (1980). *Gene*, **9**, 1–12.
Jeppesen, P. G. N. (1974). *Anal. Biochem.* **58**, 195–207.
Johnston, H. M. & Roth, J. R. (1979). *Genetics*, **92**, 1–15.
Johnston, H. M. & Roth, J. R. (1980). *J. Mol. Biol.* **145**, 713–734.
Johnston, H. M., Barnes, W. M., Chumley, F. G., Bossi, L. & Roth, J. R. (1980). *Proc. Nat. Acad. Sci., U.S.A.* **77**, 508–512.
Kasai, T. (1974). *Nature (London)*, **249**, 523–527.
Katz, L., Kingsbury, D. J. & Helinske, D. R. (1973). *J. Bacteriol.* **114**, 577–591.
Keller, E. B. & Calvo, J. M. (1979). *Proc. Nat. Acad. Sci., U.S.A.* **76**, 6186–6190.
Lawther, R. P. & Hatfield, G. W. (1980). *Proc. Nat. Acad. Sci., U.S.A.* **77**, 1862–1866.
Lewis, J. A. & Ames, B. N. (1972). *J. Mol. Biol.* **66**, 131–142.

Martin, R. G., Berberich, M. A., Ames, B. N., Davis, W. W., Goldberger, R. F. & Yourno, J. D. (1971). *Methods Enzymol.* **17B**, 3–44.

Maxam, A. M. & Gilbert, W. (1977). *Proc. Nat. Acad. Sci., U.S.A.* **74**, 560–564.

Miller, J. H. & Reznikoff, W. (1978). *The Operon*, Cold Spring Harbor Laboratories, New York.

Murray, M. L. & Hartman, P. E. (1972). *Can. J. Microbiol.* **18**, 671–681.

Oxender, D. L., Zurawski, G. & Yanofsky, C. (1979). *Proc. Nat. Acad. Sci., U.S.A.* **76**, 5524–5528.

Roth, J. R., Anton, D. N. & Hartman, P. E. (1966). *J. Mol. Biol.* **22**, 305–323.

Sanger, F., Nicklen, S. & Coulson, A. R. (1977). *Proc. Nat. Acad. Sci., U.S.A.* **74**, 5463–5467.

Shine, J. & Dalgarno, L. (1974). *Proc. Nat. Acad. Sci., U.S.A.* **71**, 1342–1346.

Steitz, J. (1979). In *Biological Regulation and Development* (Goldberger, R. F., ed.), pp. 349–399, Plenum Press, New York.

Stephens, J. C., Artz, S. W. & Ames, B. N. (1975). *Proc. Nat. Acad. Sci., U.S.A.* **72**, 4389–4393.

Winkler, M. E., Roth, D. J. & Hartman, P. E. (1978). *J. Bacteriol.* **133**, 830–843.

Yamamoto, K. R., Alberts, B. M., Benzinger, R., Lawhorne, L. & Treiber, G. (1970). *Virology*, **40**, 734–744.

Zurawski, G., Brown, K., Killingly, D. & Yanofsky, C. (1978*a*). *Proc. Nat. Acad. Sci., U.S.A.* **75**, 4271–4275.

Zurawski, G., Elseviers, D., Stauffer, G. V. & Yanofsky, C. (1978*b*). *Proc. Nat. Acad. Sci., U.S.A.* **75**, 5988–5992.